

# Mott-insulator states of ultracold atoms in optical resonators

Jonas Larson<sup>1</sup>, Bogdan Damski<sup>2</sup>, Giovanna Morigi<sup>3</sup>, and Maciej Lewenstein<sup>1,4</sup>

<sup>1</sup> *ICFO–Institut de Ciències Fotòniques, E-08860 Castelldefels, Barcelona, Spain*

<sup>2</sup> *Theory Division, Los Alamos National Laboratory, MS-B213, Los Alamos, NM 87545, USA*

<sup>3</sup> *Departament Física, Grup d'Òptica, Universitat Autònoma de Barcelona, E-08193 Bellaterra, Spain*

<sup>4</sup> *ICREA–Institució Catalana de Recerca i Estudis Avançats,*

*Pg Lluís Companys 23, E-08010 Barcelona, Spain*

(Dated: June 29, 2021)

We study the low temperature physics of an ultracold atomic gas in the potential formed inside a pumped optical resonator. Here, the height of the cavity potential, and hence the quantum state of the gas, depends not only on the pump parameters, but also on the atomic density through a dynamical a.c.-Stark shift of the cavity resonance. We derive the Bose-Hubbard model in one dimension, and use the strong coupling expansion to determine the parameter regime in which the system is in the Mott-insulator state. We predict the existence of overlapping, competing Mott states, and bistable behavior in the vicinity of the shifted cavity resonance, controlled by the pump parameters. Outside these parameter regions, the state of the system is in most cases superfluid.

PACS numbers: 03.75.Hh, 05.30.Jp, 32.80.Qk, 42.50.Vk

Ultracold atomic gases in optical lattices offer the unprecedented and unique possibility to study paradigmatic systems of quantum many-body physics [1, 2]. These systems allow one to realize various versions of Hubbard models [3], a prominent example of which is the Bose-Hubbard model [4], exhibiting the superfluid (SF) – Mott insulator (MI) quantum phase transition [5]. The realization of the Bose-Hubbard model with ultracold atoms has been proposed in the seminal theoretical work in Ref. [6], and demonstrated in the milestone experiments in Ref. [7]. Several aspects and modifications of the SF – MI quantum phase transition (or crossover [8]) are object of intense studies [2].

Optical lattices in free space are not affected by the presence of the atoms. This scenario is, however, strongly modified when the atoms move in the optical potential which is formed inside a pumped resonator: Here, the atoms interact with the cavity mode while the cavity field, determining the optical lattice, may critically depend on the density of the atoms [9, 10]. Several recent studies address Cavity Quantum Electrodynamics (CQED) with cold atoms. CQED techniques were used to measure pair correlations in the atom laser [11], and have been proposed for characterizing quantum states of ultracold matter [12]. Self-organization of atoms in transversally pumped cavities was observed in [13], and theoretically described in [14]. Bragg scattering of atomic structures inside optical resonators has been investigated in [15]. Most recently, Bose-Einstein condensed atoms have been loaded inside cavities [16]. This experimental progress calls for theoretical development of CQED combined with many-body physics.

In this Letter we determine the ground state of ultracold atomic gases in the optical lattice of a cavity. The cavity is driven by a laser, and the atoms shift the cavity resonance, thus affecting the intracavity field amplitude, which in turn determines the depth of the cavity poten-

tial and the ground state of the atomic gas itself. The problem is hence highly non-linear, as the optical lattice and state of the atoms have to be evaluated in a self-consistent way. The derivation of the corresponding Bose-Hubbard model for few atoms has been discussed by Maschler and Ritsch in Refs. [17]. In this Letter, we derive the Bose-Hubbard model in an appropriate thermodynamic limit. We study its ground state applying the strong coupling expansion [18] to calculate the boundaries of the MI states, determined by the dependence on the parameters of the system: pump strength and frequency, density of atoms, and chemical potential.

Our model consists of bosonic atoms confined in a 1D trap inside an optical resonator of a fixed length driven by a laser field. The atomic dipole transition is far-off resonance from the cavity mode, which induces a dipole potential acting on the atoms. Using the notation of [17], the single-particle Hamiltonian reads:

$$\hat{H}_0 = \frac{\hat{p}^2}{2m} + \hbar [U_0 \cos^2(k\hat{x}) - \Delta_c] \hat{n}_{\text{ph}} - i\hbar\eta (\hat{a} - \hat{a}^\dagger). \quad (1)$$

Here,  $\hat{p}$ ,  $\hat{x}$  and  $m$  are the atomic momentum, position, and mass,  $\eta$  is the amplitude of the pump at frequency  $\omega_p$ ,  $\Delta_a = \omega_p - \omega_a$  and  $\Delta_c = \omega_p - \omega_c$  are the detunings of the pump from atom and cavity frequencies,  $k = \omega_c/c$  is the mode wave vector,  $\hat{a}^\dagger$  and  $\hat{a}$  are the creation and annihilation operators of a cavity photon of energy  $\hbar\omega_c$ , and  $\hat{n}_{\text{ph}} = \hat{a}^\dagger\hat{a}$  is the number of photons. The depth of the single-photon dipole potential is  $U_0 = g_0^2/\Delta_a$ , where  $g_0$  is the atom-cavity mode coupling. The many-body Hamiltonian is obtained from Eq. (1) including the atomic contact interactions; it is conveniently represented in second-quantized form with the atomic field operators  $\hat{\Psi}(x)$ ,  $\hat{\Psi}^\dagger(x)$  obeying the bosonic commutation relations. We assume the bad-cavity limit, where the resonator field reaches the stationary state on a faster time scale than the one of the atomic dynamics, and eliminate the cav-

ity field from the equations of the atomic operators. In this limit the amplitude of the intracavity field depends non-linearly on the atomic fields through the operator  $\hat{\mathcal{Y}} = \int dx \cos^2(kx) \hat{\Psi}^\dagger(x) \hat{\Psi}(x)$ , and reads

$$\hat{a}(\hat{\mathcal{Y}}) = \frac{\eta}{\kappa - i(\Delta_c - U_0 \hat{\mathcal{Y}})}, \quad (2)$$

where  $\kappa$  is the cavity damping rate. Correspondingly, the Heisenberg equation for the atomic field operator reads

$$\dot{\hat{\Psi}} = -\frac{i}{\hbar} [\hat{\Psi}(x), \hat{\mathcal{H}}_0] - i\hat{\mathcal{C}}(\hat{\mathcal{Y}}, x), \quad (3)$$

where  $\hat{\mathcal{H}}_0 = \int dx \hat{\Psi}^\dagger(x) \left( -\frac{\hbar^2 \nabla^2}{2m} + \frac{u}{2} \hat{\Psi}^\dagger(x) \hat{\Psi}(x) \right) \hat{\Psi}(x)$ , with  $u$  being the strength of the contact interaction, and

$$\hat{\mathcal{C}}(\hat{\mathcal{Y}}, x) = U_0 \cos^2(kx) \hat{a}^\dagger(\hat{\mathcal{Y}}) \hat{\Psi}(x) \hat{a}(\hat{\mathcal{Y}}) \quad (4)$$

which arises from keeping track of the correct normal ordering of atomic and photonic field operators. Starting from Eq. (3), the derivation of the Bose-Hubbard Hamiltonian is not straightforward due to the form of operator (4). This is evident when expanding the atomic field operators, assuming the validity of the tight-binding approximation (TBA) and the occupation of the lowest energy band:  $\hat{\Psi}(x) = \sum_i w(x-x_i) \hat{b}_i$ , where  $\hat{b}_i$  and  $w(x-x_i)$  are the atomic annihilation operator and Wannier function at site  $i$ , respectively. The Wannier functions depend on  $\hat{\mathcal{Y}}$  and, therefore, on the number of atoms  $N$  or, equivalently, on the atomic density, which in turn depends on Wannier functions. Moreover, the commutation relation  $[\hat{b}_i, \hat{b}_j^\dagger] = \delta_{ij}$  is valid only in the lowest order in the expansion in  $1/N$ . In effect, the Wannier expansion must be performed self-consistently in the thermodynamic limit, by letting  $N$  and the cavity volume to infinity, keeping finite the number of atoms per potential site. Additionally, we impose  $U_0 = u_0/N$  and  $\eta = \eta_0 \sqrt{N}$ , where  $u_0$  and  $\eta_0$  are constants, which corresponds to keeping the depth of the cavity potential  $V = \hbar U_0 n_{\text{ph}}$  constant as  $N$  is increased. The Bose-Hubbard Hamiltonian  $\hat{H}$  is obtained discarding couplings beyond nearest-neighbor. Its rescaled form  $\hat{\tilde{H}} = \hat{H}/U$ , with  $U$  the strength of the on-site interaction, reads

$$\hat{\tilde{H}} = -\tilde{t} \hat{B} + \frac{1}{2} \sum_i \hat{n}_i (\hat{n}_i - 1) - \tilde{\mu} \hat{N}, \quad (5)$$

where  $\hat{N} = \sum_i \hat{n}_i = \sum_i \hat{b}_i^\dagger \hat{b}_i$  is the atom number operator and  $\hat{B} = \sum_i \hat{b}_i^\dagger \hat{b}_{i-1} + \text{h.c.}$  is the hopping term. The term  $\tilde{\mu} = \frac{\mu}{U} + \frac{f(\hat{N})}{NU}$  contains the rescaled chemical potential, where the second term is a constant in the thermodynamic limit. The tunneling parameter

$$\tilde{t} = -\frac{E_1}{U} - \frac{\hbar \eta^2 U_0 J_1}{U(\kappa^2 + \zeta^2)} \quad (6)$$

is expressed in terms of  $\zeta = \Delta_c - u_0 J_0 \hat{n}_0$  and of the coefficients  $U = u/2 \int dx |w(x)|^4$ ,  $E_\ell = \int dx w(x-x_i) (-\hbar^2/2m) (d^2/dx^2) w(x-x_{i+\ell})$  and  $J_\ell = \int dx w(x-x_i) \cos^2(kx) w(x-x_{i+\ell})$ , with  $\ell = 0, 1$ . Note that  $\hat{N}$ , and hence the atomic density in the homogeneous case, is a conserved quantity since  $[\hat{N}, \hat{H}] = 0$ . In deriving Eq. (5) we have used that  $J_1 \ll J_0$ . The higher order terms in  $J_1 \hat{B}$ , describing long-range interactions, have hence been neglected. We note that the parameters  $\tilde{\mu}$  and  $\tilde{t}$  depend on the atomic density through the Wannier functions, and at the same time determine the state of the system, and in particular the density: This is a genuine CQED effect, where the non-linearity of the coupling between photons and atoms depends on the atom number. As a consequence, the atomic density in this system is not determined by the chemical potential alone.

From Eq. (5) we determine the parameter regimes of the MI states using the strong coupling expansion [18]. Here, the boundaries of the MI regions are determined by comparing the energy of the MI state, given by  $n_0$  atoms at each site of the periodic potential, with the corresponding energies of the excited states with one additional or missing particle (particle and hole states). This procedure involves the evaluation of the Wannier functions for all cases. As the coefficients of the Bose-Hubbard Hamiltonian both depend on and determine the atomic density, the Wannier functions have to be calculated self-consistently. This is done by solving the non-linear equation in presence of the potential  $V = \hbar U_0 n_{\text{ph}} = \hbar u_0 \eta_0^2 / \left[ \kappa^2 + (\Delta_c - u_0 J_0 n_0)^2 \right]$ , where  $J_0$  is an integral of Wannier functions. This equation cannot be solved by iteration, as one encounters periodic doubling bifurcations and deterministic chaos. We solve it numerically by checking for self-consistent solutions, using the Gaussian approximation of the Wannier functions, and thus approximating  $w(x) \approx \exp(-x^2/2\sigma^2)/(\sqrt{\pi}\sigma)^{1/2}$  where  $\sigma$  is the parameter to be determined [19]. In terms of the dimensionless quantity  $y = k^2 \sigma^2$ , giving the extension of the Gaussian wave packet in units of the cavity mode wavelength, the problem can be reduced to solving self-consistently the equation  $J_0(y) = \frac{1}{2} (1 - d_a e^{-y})$ , where  $d_a$  is the sign of the detuning  $\Delta_a$ . For a given set of parameters, multiple (bistable [20]) solutions appear when the number of photons is maximum, namely when the denominator of Eq. (2) is minimum, which occurs at the shifted resonance

$$\Delta_c - u_0 J_0 n_0 = 0. \quad (7)$$

Since the sign of  $u_0$  is determined by the detuning  $\Delta_a$ , Eq. (7) allows for real solutions only when  $\Delta_a$  and  $\Delta_c$  have the same sign: Then, the resonance condition depends on the number of atoms. Correspondingly, the cavity is driven at resonance, the number of photons reaches the maximum value  $n_{\text{ph}} = \eta^2/\kappa^2$ , and the cavity potential is the deepest. An important distinction must be

made between the cases  $\Delta_a > 0$  ( $U_0 > 0$ ) and  $\Delta_a < 0$  ( $U_0 < 0$ ): In the first case, the potential minima are at the nodes of the standing wave, where the intracavity field vanishes. Strong localization of the atoms at these points implies that the coupling of the atoms with the field is minimum,  $J_0 \rightarrow 0$ . The quantum fluctuations give rise to a finite coupling, determining the quantum state. On the contrary, when  $\Delta_a < 0$  the potential minima are at the antinodes of the standing wave, where the intracavity field is maximum. Strong localization of the atoms at these points implies strong coupling with the field, with  $J_0 \rightarrow 1$ . In this regime, CQED effects are expected to play a dominant role.

We plot the boundaries of the resulting Mott states in the  $\tilde{\mu} - \eta^{-1}$  plane, i.e., the effective chemical potential and the inverse of the pump strength. Here, large pump strengths correspond to deep optical potentials, hence to vanishing tunneling,  $t \rightarrow 0$ . The physical system we consider is a gas of  $^{87}\text{Rb}$  atoms with scattering length  $a_s = 5.77$  nm, whose dipole transition at wavelength  $\lambda = 830$  nm couples to the mode of a resonator at decay rate  $\kappa = 2\pi \times 100$  kHz. The potential has transverse size  $\Delta_y = \Delta_z = 30$  nm and  $K$  sites in the longitudinal axis. We evaluate the "phase diagrams" for  $K = 50 - 10000$  at fixed number of atoms  $N$ , scaling  $N$  so to keep the atomic density constant. The results for the Mott zones agree over the whole range of values, so in the figures we report the ones obtained for  $K = 50$ .

We first discuss the case in which the detunings  $\Delta_a$  and  $\Delta_c$  have different signs, i.e., far from bistability [20] when Eq. (7) is not fulfilled. As expected, there is a peculiar difference between the cases  $\Delta_a > 0$  (atoms at the nodes) and  $\Delta_a < 0$  (atoms at the antinodes): When  $\Delta_a < 0$ , in the tight-binding regime  $J_0 \rightarrow 1$  and thus  $V \propto 1/(\kappa^2 + (\Delta_c + n_0 u_0)^2)$ . Hence, the dependence on the atomic density is strongest. In Fig. 1(a) the MI zones are displayed. The shapes are similar to the standard ones [18], apart from the region  $\eta \rightarrow \infty$  where, despite being out of the bistable regime [20], the lobes considerably overlap. This effect is due to the competition between the non-linear coupling to the cavity field, giving the depth of the potential, and the strength of the on-site interactions, affecting the number of atoms per site  $n_0$ . In the other case,  $\Delta_a > 0$ , one has  $J_0 \ll 1$ . For  $\eta \rightarrow \infty$ , then  $J_0 \rightarrow 0$ , the cavity potential depth is almost independent of  $n_0$  and one obtains the standard Bose-Hubbard Hamiltonian. For large but finite values of  $\eta$ , however,  $J_0$  is finite and the dependence of the coefficients on  $n_0$  becomes relevant. Figure 1(b) shows the "phase diagram" for  $|U_0| = 2\kappa$  and  $\Delta_c = 0$ . Here, the MI regions exhibit a regular behavior at  $\eta \rightarrow \infty$ . As  $\eta$  is decreased they start to overlap and become disconnected. This behaviour introduces two new critical points at the tips of the disconnected regions, whose nature will be studied in future works. We note that the MI zones enter the region of negative  $\tilde{\mu}$ . The minima of  $\tilde{\mu}$  are at the

pump values where the on-site repulsion is balanced by the effective potential  $V$ .

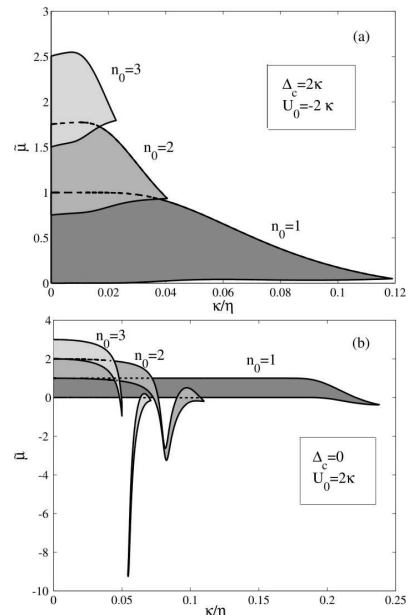


Figure 1: Boundaries of MI regions as a function of the rescaled chemical potential  $\tilde{\mu}$  and the inverse of the pump strength  $\eta$  (in units of  $\kappa$ ) for (a)  $\Delta_c = 2\kappa$  and  $U_0 = -2\kappa$  and (b)  $\Delta_c = 0$  and  $U_0 = 2\kappa$ ;  $n_0$  denotes the site occupation in the 1D cavity lattice potential of  $K = 50$  sites. The dashed lines show the boundaries of the zones which are hidden.

We now consider the situation when  $\Delta_a$  and  $\Delta_c$  have the same sign, such that Eq. (7) may have real solutions. From Eq. (7), for  $n_0 = 1$  and  $U_0 = -\kappa$  we find bistable behavior for  $J_0 = |\Delta_c|/50\kappa$  and  $J_0$  sufficiently close to 1, which is fulfilled for instance for  $\Delta_c = -45\kappa$ . The corresponding diagram is displayed in Fig. 2. The inset shows the potential  $V$  as a function of  $\eta$  for  $n_0 = 1$ . Here, one encounters a bistability point while lowering the pump intensity, where the cavity field potential discontinuously jumps to a second branch with  $|V| \ll E_r$ ,  $E_r = \hbar^2 k^2 / 2m$  being the recoil energy. The first branch corresponds to the left MI-region of the phase diagram at  $n_0 = 1$ . In the second branch, instead, the TBA is not valid, hence most probably the atomic gas will no longer be in the lowest band of the cavity potential, and rather definitely no longer in a MI state. Using both Gaussian and Wannier functions we have verified that our treatment breaks down as soon as the system goes out from the MI region on the left of Fig. 2. This instability has the character of a first order transition. The right MI region in Fig. 2 is found by applying the theory of [18]. It occurs at values of  $\eta$  for which  $|V|$  is in the second branch, and is thus of dubious validity, since here the TBA breaks down. Instability leads here apparently to population of higher Bloch bands; most probably the true ground state in this regime is SF (BEC in a very weak lattice potential). Let us conjecture that we could find parameter

regions where the cavity potential for both branches of solutions would support the TBA. In that case, at a given density there would exist two stable values of the tunneling and onsite-interaction matrix elements. Then, for a fixed  $\tilde{\mu}$  we would have two possible phases, of which only one will be energetically favorable, but both being by construction stable with respect to small perturbations, such as single particle or hole excitations.

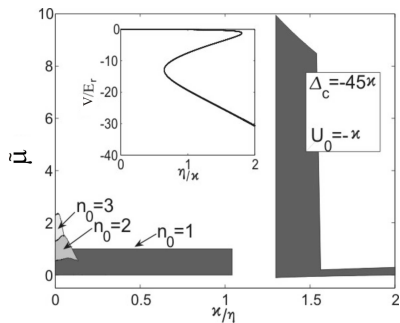


Figure 2: Phase diagram showing the MI regions for  $\Delta_c = -45\kappa$  and  $U_0 = -\kappa$ . Inset:  $V$  (in units of  $E_r$ ) as a function of  $\eta$  for  $n_0 = 1$ . The bistability causes the system to go out of the left MI region with  $n_0 = 1$ . The right MI-region for  $n_0 = 1$  is an artifact of the theory [18], as here the TBA is invalid.

So far we have considered a fixed number of atoms. If instead the system is coupled to an atomic reservoir, and the number of atoms is hence not fixed, then a change of the system parameters can lead either to continuous or to abrupt changes of the atomic density, and hence of the ground state, analogue to second- and first-order phase transitions, respectively. When the parameters are such, that the system does not exhibit bistability, then  $\tilde{\mu}$ ,  $\kappa/\eta$  and the atomic density determine uniquely the coefficients in the Bose-Hubbard model and the ground state. In the case of overlapping MI zones, as in Fig. 1(a), the system would relax to the state with the density which minimizes the energy. Nonetheless, by slowly changing  $\tilde{\mu}$ , corresponding to spanning the phase diagram along the ordinate, we expect hysteresis in the atomic on-site density, since the states inside the Mott correspond to local energy minima. Note that such local changes of on-site  $\tilde{\mu}$  are also encountered when the system is inhomogeneous, for instance, in presence of a harmonic trap. The atomic density will exhibit then the characteristic "wedding cake" form (cf. [2, 6, 8]). Sufficiently slow changes of the trap frequency should then lead to hysteresis in the "wedding-cake" shape. Applications of this effect could include many-body quantum switches and generation of coherent superpositions of Mott states.

This letter refers to the case, in which the atomic density globally affects the cavity field. Situations, when the atoms may affect locally the cavity field, can be found in multimode resonators [21, 22]. In these scenarios one could find features typical of phonon-like

physics in solid state. We acknowledge discussions with I. Bloch, T. Esslinger, S. Fernandez, Ch. Maschler, H. Monien, E. Polzik, J. Reichel, and H. Ritsch, and support from the Swedish government/Vetenskapsrådet, the German DFG (SFB 407, SPP 1116), the EU commission (SCALA, Contract No. 015714), ESF PESC QUEDIS, the US Department of Energy, and the Spanish MEC (FIS2005-04627, Ramon-y-Cajal, Consolider Ingenio 2010 "QOIT").

- 
- [1] I. Bloch and M. Greiner, *Adv. At. Molec. Opt. Phys.* **52**, 1 (2005).
  - [2] M. Lewenstein *et al.*, *Adv. Phys.* **56**, 243 (2007).
  - [3] D. Jaksch and P. Zoller, *Ann. Phys. (N.Y.)* **315**, 52 (2005).
  - [4] M.P.A. Fisher, P.B. Weichman, G. Grinstein, and D.S. Fisher, *Phys. Rev. B* **40**, 546 (1989).
  - [5] S. Sachdev, *Quantum Phase Transitions* (Cambridge University Press, Cambridge, 1999).
  - [6] D. Jaksch *et al.*, *Phys. Rev. Lett.* **81**, 3108 (1998).
  - [7] M. Greiner *et al.*, *Nature* **415**, 39 (2002).
  - [8] G.G. Batrouni *et al.*, *Phys. Rev. Lett.* **89**, 117203 (2002); G.G. Batrouni *et al.*, *Phys. Rev. A* **72**, 031601(R) (2005).
  - [9] P. Domokos and H. Ritsch, *J. Opt. Soc. Am. B* **20**, 1098 (2003).
  - [10] This property can allow to reproduce the physics resulting from electron-phonon interactions in condensed-matter, such as Peierls instability, or magnetization plateaux, cf. T. Vekua *et al.*, *Phys. Rev. Lett.* **96**, 117205 (2006), and references therein.
  - [11] A. Öttl, S. Ritter, M. Köhl, and T. Esslinger, *Phys. Rev. Lett.* **95**, 090404 (2005).
  - [12] I. B. Mekhov, C. Maschler, and H. Ritsch, *Nature Physics* **3**, 319 (2007); W. Chen, D. Meiser, and P. Meystre, *Phys. Rev. A* **75**, 023812 (2007).
  - [13] A.T. Black, H.W. Chan, and V. Vuletić, *Phys. Rev. Lett.* **91**, 203001 (2003).
  - [14] P. Domokos and H. Ritsch, *Phys. Rev. Lett.* **89**, 253003 (2002); J.K. Asbóth, P. Domokos, H. Ritsch and A. Vukics, *Phys. Rev. A* **72**, 053417 (2005).
  - [15] S. Slama *et al.*, *Phys. Rev. Lett.* **94**, 193901 (2005).
  - [16] S. Slama, *et al.*, *Phys. Rev. A* **75**, 063620 (2007); P. Treutlein, *et al.*, *Phys. Rev. Lett.* **99**, 140403 (2007); F. Brennecke, *et al.*, *Nature* **450**, 268 (2007); Y. Colombe, *et al.*, *Nature* **450**, 272 (2007).
  - [17] C. Maschler and H. Ritsch, *Phys. Rev. Lett.* **95**, 260401 (2005). C. Maschler, I. Mekhov, and H. Ritsch, arXiv:0710.4220.
  - [18] J.K. Freericks and H. Monien, *Europhys. Lett.* **26**, 545 (1994); *Phys. Rev. B* **53**, 2691 (1996).
  - [19] We use modified functions from a Gaussian ansatz, satisfying orthogonality between neighbouring sites.
  - [20] R. Bonifacio and L. A. Lugiato, *Phys. Rev. Lett.* **40**, 1023 (1978); *Phys. Rev. A* **18**, 1129 (1978).
  - [21] M. Lewenstein *et al.*, in *Atomic Physics 20*, ed. by C.F. Roos, H. Häfner, and R. Blatt, (AIP Proceedings, Melville, 2006), **869**, pp. 201-211.
  - [22] D. Meiser and P. Meystre, *Phys. Rev. A* **74**, 065801 (2006).